Agricultural and Forest Meteorology 271 (2019) 193–206

Contents lists available at ScienceDirect

Agricultural and Forest Meteorology

journal homepage: www.elsevier.com/locate/agrformet

N_2O flux short-term response to temperature and topsoil disturbance in a fertilized crop: An eddy covariance campaign

M. Lognoul[a,*], A. Debacq[a], A. De Ligne[a], B. Dumont[b], T. Manise[b], B. Bodson[b], B. Heinesch[a], M. Aubinet[a]

[a] Exchanges Ecosystems—Atmosphere, TERRA Teaching and Research Centre, Gembloux Agro-Bio Tech, University of Liège, Belgium
[b] AgroBioChem Dept., Gembloux Agro-Bio Tech, University of Liège, Belgium

ARTICLE INFO

Keywords:
Nitrous oxide
Eddy covariance
Sugar beet
Crops
Fertilization
Soil disturbance
Temperature

ABSTRACT

Using the eddy covariance technique, half-hourly N_2O fluxes were measured over a sugar beet crop (ICOS Station, Lonzée, BE) from fertilization to harvest. Several parameters of the data quality control tests were adapted to suit the characteristics of N_2O. No u* filtering threshold could be seen for N_2O fluxes; therefore, it was determined based on CO_2 data. The uncertainty of N_2O fluxes was assessed for several aspects of data treatment (total random uncertainty, spectral correction, u* filtering, gap-filling), which were combined to determine the uncertainty of the N_2O budget.

Between fertilization and harvest, the crop emitted 1.83 (± 0.21) kg N_2O-N ha^{-1} corresponding to 1.2% of N supplies. Flux variability was characterized by three episodes of high emissions across the experiment, interspersed with lower background fluxes. These peak events were driven by soil moisture and temperature, dependent on the time-scale. Soil water content at 5 cm was identified as the single trigger for N_2O emission peaks given sufficient N availability, while intraday oscillations were positively correlated to the variations in surface temperature rather than deeper soil temperatures.

For the first time, an inhibiting and short-term effect of topsoil disturbance (seed-bed preparation) on N_2O fluxes was recorded, which interrupted the peak that followed fertilization, and delayed the start of the next high emission episode. This observation, along with the synchronicity found between surface temperature and diel oscillations of N_2O fluxes, supports the hypothesis of a N_2O-producing microbial community located in the topmost soil layer. Given that a third of the overall N_2O emissions during the measurement campaign occurred between fertilization and seed-bed preparation, further investigation into the timing of farming operations as mitigation strategies is needed.

The contribution of N_2O emissions to the net greenhouse gas balance (which comprises CO_2 and N_2O fluxes) was estimated at between 20 and 66%. Our results stress the importance of including nitrous oxide when measuring gas exchanges in fertilized crops, and to do so at high temporal resolution for improved estimates.

1. Introduction

Nitrous oxide (N_2O) is a long-lived greenhouse gas (GHG) considered to be the third largest contributor to global warming (Ciais et al., 2013) and a major factor in stratospheric ozone depletion (Portmann et al., 2012). The agricultural sector contributes 72.2% of European Union N_2O emissions (Mandl et al., 2018). N_2O atmospheric concentration reached 330 nmol mol^{-1} in 2017 (NOAA (National Oceanic and Atmospheric Administration), 2018) and the estimated growth of 0.80 nmol mol^{-1} per year is mainly explained by an intensified use of nitrogen fertilizers (Ussiri and Lal, 2013). In Belgium, 33.7% of agricultural GHG emissions originate from N_2O produced by soils (IRCEL (Belgian Interregional Environment Agency), 2017). Although national estimates show a 24% decrease for the period between 1990 and 2014, N_2O emissions rates were predicted to increase by 3 kgN_2O-N ha^{-1} every year between 1990 and 2050 (Roelandt et al., 2007).

In agricultural lands, N_2O mostly originates from microbial nitrifying and denitrifying processes occurring in soil (Bracker and Conrad, 2011). The basic substrates for nitrification and denitrification are ammonium and nitrate (respectively acting as electron donor and acceptor), and N availability in soils correlates with N_2O production

* Corresponding author.
E-mail address: margaux.lognoul@uliege.be (M. Lognoul).

https://doi.org/10.1016/j.agrformet.2019.02.033
Received 16 October 2018; Received in revised form 21 February 2019; Accepted 23 February 2019

(Conrad, 1996). Labile C also plays a role in these processes as a source of C for heterotrophic nitrifiers and denitrifiers (Groffman and Robertson, 2007). N_2O biotic production is driven by pedo-climatic conditions, dependent on weather and farming practices (Ussiri and Lal, 2013). N_2O fluxes are usually characterized by high temporal variability with emission bursts (known as "hot moments") interspersed with low background fluxes (Butterbach-Bahl et al., 2013; Molodovskaya et al., 2012). Spatial variability was also observed (with "hot spots") in agricultural ecosystems (Hénault et al., 2012), due to heterogeneous soil physicochemical properties (Mathieu et al., 2006) and uneven distributions of microbial abundance (Jahangir et al., 2011).

Given sufficient N availability, N_2O emission bursts can be triggered under high soil water content following precipitation (Castellano et al., 2010; Plaza-Bonilla et al., 2014), irrigation (Trost et al., 2013) or freeze-thaw events (Ludwig et al., 2004). Such emission peaks are usually observed after fertilization, although peaks attributed to organic matter mineralization several months after N input are also documented (Lognoul et al., 2017).

Soil temperature plays a role in N_2O emissions by influencing microbial activity (Flechard et al., 2007). Moreover, increasing temperatures, by stimulating soil respiration, can result in greater anaerobic zones that are favorable to denitrification (Smith et al., 2003). Short time-scale variations are not well understood: a positive diel correlation between N_2O emissions and soil surface temperature was observed by Laville et al. (2011) over a very short period of time (9 days), while negative correlations were also recorded (Shurpali et al., 2016). Alves et al. (2012) reported a positive relationship with temperature deeper in the soil profile.

Regarding farm management and soil disturbance, mainly tillage practices have been studied in relation to N_2O emissions, especially their long-term effects (D'Haene et al., 2008; Drury et al., 2006; Vian et al., 2009). When compared with practices involving ploughing, reduced tillage tends to enhance N_2O emissions in the long term (Abdalla et al., 2013) by concentrating crop residues in the uppermost soil layer and favoring microbial development (Lognoul et al., 2017). However, the short-term effect (daily to monthly scales) of soil disturbance is rarely investigated, mostly because of a lack of sufficient temporal resolution due to limiting measurement techniques. In particular, to our knowledge the short-term effect on N_2O fluxes of soil disturbance by seedbed preparation in croplands has not yet been studied.

Up to now, most *in situ* studies on crops were performed using manual closed chambers at low temporal resolution. However, this technique prevents researchers from adequately capturing the sudden variations in N_2O emissions (Kroon et al., 2008) and can be source of error when measurements are scaled up spatially (Lammirato et al., 2018). Automated chambers that allow an improved temporal resolution have also been used (Laville et al., 2011, Theodorakopoulos et al., 2017), but the uncertainty related to spatial variability remains. The eddy covariance (EC) technique represents a suitable alternative because it can provide continuous flux estimates at high resolution (half-hourly scale) integrated over a large surface area (Aubinet et al., 2012), thus obviating spatial heterogeneity. However, the EC data treatment typically used for CO_2 and H_2O needs to be adjusted for N_2O. This includes reviewing parameters of quality tests and determining the time-lag, which can be challenging when the signal-to-noise ratio is low (Langford et al., 2015). It is only recently that a reference document concerning non$-CO_2$ gases was published by the European network ICOS (Nemitz et al., 2018).

On the whole, the main drivers of N_2O exchange have been identified. However, it remains unclear how the driving variables affect fluxes in terms of amplitude and timescale, and how they are influenced by crop management. These knowledge gaps and low-precision budget estimates make it difficult to implement mitigation guidelines for farmers. Therefore we set up an eddy covariance measurement campaign on a managed cropland with the aim to (1) determine the appropriate EC data treatment for our N_2O dataset, (2) assess the short-term response of N_2O fluxes to farming practices together with meteorological variables *in situ,* and (3) estimate the N_2O budget of a production crop, and its uncertainty, from fertilization to harvest.

2. Materials and methods

2.1. Study site

The study site is a 12 ha crop field located in the Lonzée Terrestrial Observatory (Level-2 ICOS Station) in central Belgium. The site has been cultivated for at least 80 years. It is owned and managed by a local farmer, and is subject to a 4-year rotation: winter wheat (*Triticum aestivum* L.) / sugar beet (*Beta vulgaris* L.) / winter wheat (*Triticum aestivum* L.) / seed potato (*Solanum tuberosum* L.). The climate is oceanic temperate (mean annual temperature: 10.2 °C, annual precipitation: 743 mm). The soil is characterized by a silt-loam texture (FAO classification: Luvisol) with 20% clay, 7.5% sand, and 72.5% silt. A detailed description of the site can be found in Moureaux et al. (2006).

The present study was conducted from March to October 2016, focusing on a sugar beet crop which represents the second most important root crop in Belgium and in Europe (StatBel, 2018). To our knowledge, it is the first EC dataset collected for N_2O on this type of crop. The sequence of farming operations is reported in Table 1. The application of N fertilizer was performed 22 days before seeding. It is usually recommended to wait at least 10 days to avoid excessive ammonium soil concentrations that can be toxic for germinating seedlings (Laudinat, 2015). Seeding was itself preceded by a seed-bed preparation the day before, to level the soil surface and break up aggregates to favor plant emergence.

The sugar beet crop in this study was preceded by winter wheat (October 2014 to August 2015). A mustard cover crop was established between the two main crops (August to December 2015).

Table 1
Calendar of farming operations during the experiment.

Date	Farming operations	Specifications
07-Dec-2015	Winter ploughing	Over mustard using a moldboard plow (30-cm depth)
22-Mar-2016	Liquid nitrogen application	NH_4NO_3 (136.5 kg N ha^{-1})
9-Apr-2016	Weeding	Glyphosate (972 g ha^{-1})
12-Apr-2016	Seed-bed preparation	Stubble cultivator followed by a rotary harrow (7 to 10 cm depth)
13-Apr-2016	Sugar beet sowing	Row drilling of *Beta Vulgaris* L. cv Lisanna KWS
3-9-19-May-2016 23-Jun-2016	Weeding	Phenmedipham, ethofumesate, metamitron, triflusulfuron-methyl, dimethenamid-P
11-Jun-2016	Urea application	4 kg N ha^{-1}
1-14-Aug-2016	Fungicide application	Epoxyconazole, fenpropomorph, pyraclostrobin
27-Oct-2016	Harvest	Yield of 83 ton ha^{-1} (16% sugar)
29-Oct-2016	Ploughing and soil preparation Winter wheat sowing	/

2.2. Measurement system

2.2.1. Meteorological and ancillary measurements

Meteorological conditions were monitored by a weather station located in the center of the field. The station was equipped with a radiometer measuring global and net radiation (CNR4, Kipp and Zonen, Delft, NL) and photo-receptor cells measuring photosynthetic photon flux density (PAR Quantum sensor SKP 215, Skye Instruments Limited, Llandrindod Wells, UK). A weighing rain gauge (TRw S415, MPS system s.r.o., Bratislava, SK) recorded precipitation. Air temperature and humidity were measured by a thermistor and an electrical capacitive hygrometer (RHT2nl, Delta-T Devices Ltd, Cambridge, UK). An infrared remote temperature sensor (IR 120, Campbell Scientific, Logan, UT, US) monitored the surface temperature. This temperature was considered to be the canopy temperature once the leaf area index (LAI) exceeded 0.5 $m^2_{leaf} m^{-2}_{soil}$, corresponding to a canopy height of 15 cm.

In addition, pedoclimatic conditions were monitored at 5, 15, and 25 cm depth for three locations around the station to derive averages for each depth. The ground instrumentation included electrical resistance thermometers for soil temperature (PT 107, Campbell Scientific, Logan, UT, US) and time domain reflectometers for soil moisture (EnviroSCAN-Probe, Sentek Sensor Technologies, Stepney, SA, Australia).

The LAI was determined by regular destructive sampling in six subplots from the beginning of June to October. Green leaves were cleaned and air-dried, then scanned to determine their surface area, which was divided by the sampling area.

2.2.2. Flux measurements

N_2O and CO_2 fluxes were measured continuously at the field scale using the eddy covariance technique (Aubinet et al., 2012). The eddy covariance tower and related instruments were located in the center of the field. The CO_2 concentration was measured at 10 Hz by an infrared gas analyzer (LI-7200, LI-COR, Lincoln, NE, US). Flux calculations and data treatments for CO_2 are described in Buysse et al. (2017).

The N_2O concentration was measured at 10 Hz using a quantum cascade laser (QCL) spectrometer controlled by the TDLWintel data acquisition program (Aerodyne Research Inc., Billerica, MA, USA). H_2O concentration was also measured by the instrument. Air sampling was ensured by a vacuum pump downstream (TriScroll 600 Dry Scroll Pump, Agilent Technologies, Santa Clara, CA, USA) and through a 8.2 m long and 4.5 mm wide sampling tube upstream of the QCL. The tube was equipped with an inlet rain cap (Intake Tube Rain Cap V3, LI-COR, Lincoln, NE, USA) and protected by insulating foam traversed by a heating resistor. The flow and cell pressure were controlled by a needle valve at the inlet of the sampling cell. The cell pressure was set at 26.7 hPa with a nominal flow rate of 6 standard l/min. This low pressure helps to limit collisional broadening in the spectrometer but does not eliminate it (Mappe Fogain, 2013). Therefore, the data acquisition program computes the dry mixing ratio of N_2O using a built-in correction, accounting for gas dilution and pressure broadening caused by the presence of water vapor. However, a residual cross-talk between H_2O and N_2O could persist and affect very low fluxes (Nemitz et al., 2018). Verification was done on small N_2O fluxes (< 0.3 nmol $m^{-2} s^{-1}$), which were grouped by class of temperature (class range: 2.5 °C) to obviate a potential co-dependency of N_2O and H_2O on this variable, and the correlation between the two gases was tested. No significant relationship was found for any of the temperature classes; the correction performed by TDLWintel was thus considered sufficient for our experiment.

The temperature of the sampling cell was maintained at 25 °C using a 20% ethanol-fluid recirculating chiller (OASIS THREE chiller, Solid State Cooling, Wappingers Falls, NY, USA). Wind tridimensional velocities were measured at 20 Hz by a sonic anemometer (Solent Research HS-50, Gill Instruments, Lymington, UK). The inlet of the sampling tube and the anemometer were both mounted on the tower at 2.8 m height above ground, with a 19.7 cm separation (eastward separation: 18.9 cm; southward separation: 6.8 cm; no vertical separation).

2.3. N_2O flux computation

The computation of half-hourly fluxes was performed using the eddy covariance processing software EddyPro® (LI-COR Environmental, LI-COR, Lincoln, NE, USA).

Means were calculated using block averaging over 30 min. As recommended by ICOS (Sabbatini et al., 2016), the planar fit method (Wilczak et al., 2001) was used to rotate the anemometer coordinates. When compared to the double rotation, the two methods correlated very well ($R^2 = 0.99$) with a slope of 1.01.

The time-lag between the data streams of the N_2O mixing ratio and vertical wind velocity was determined by searching for the maximum of the covariance function in a narrow time window, for which limits ([0.9–3.0] s) were assessed by a visual examination of the frequency distribution of time-lags in a larger window (20 s) for the entire data set (see Figure S1 in Supplement). 62% of time-lags fell into the narrow time window. It should be noted that even during periods of low fluxes (< 0.5 nmol $m^{-2} s^{-1}$), valuable time-lags that fell into the narrow frame window were found. If no covariance maximum could be found within such frame, a default value was applied, corresponding to the mode of the frequency distribution (1.9 s).

The season-averaged cospectrum of N_2O was compared to the cospectrum of temperature which was considered to be ideal (Foken et al., 2012). A loss of high frequency information was clearly identified (Fig. 1). A suiting correction that accounted for low-pass filtering was thus applied to N_2O fluxes. We performed the two-part method suggested by EddyPro®. This combines by multiplication two spectral correction factors, compensating respectively for losses due to sensor separation (Horst and Lenschow, 2009) and for those due to the sampling tube (Fratini et al., 2012).

The correction by Fratini et al. (2012) is based on the comparison of temperature and N_2O power spectra to derive the experimental transfer function. A Lorentzian curve is then fitted to that function between 0.005 and 0.5 Hz, for which we found a cut-off frequency of 0.11 Hz. For both stable and unstable conditions, the method selects good quality power spectra ($n_{unstable} = 86$, $n_{stable} = 77$) to calculate a linear relationship between spectral correction factors (SCF) and half-hourly averaged wind speeds. The linear model is then used to correct the rest of the dataset by retrieving SCF based on the wind speed of individual half-hours. The quality criteria for selecting good power spectra are given in Table 2. The confidence bounds of the regression were used to assess the uncertainty related to the spectral correction (see Section 2.6).

Finally, storage fluxes were assumed to be negligible at the experimental site. The storage term is usually small in short ecosystems like croplands and it is frequently measured by the one-point method rather than by profile integration (Moureaux et al., 2012). De Ligne (2018) validated this assumption for our experimental site after conducting a two-week experiment on winter wheat. They compared a three-level profile (0.1, 0.8 and 2.4 m) of CO_2 concentration measurements with the one-point method (2.4 m) and concluded that profile integration was not needed, given the low weight of storage fluxes. This was verified for N_2O fluxes on sugar beet: 95% of storage fluxes calculated with the one-point method amounted to less than 1% of total fluxes (EC flux + storage flux) and the storage term integrated over the crop season accounted for less than 0.5% of the N_2O budget.

2.4. Data quality control

2.4.1. Maintenance and statistical tests

Half-hour fluxes were discarded during periods of instrument maintenance (*e.g.* change of filter). Whenever the QCL shut down and was restarted (mainly after power cuts), the laser tuning rate took

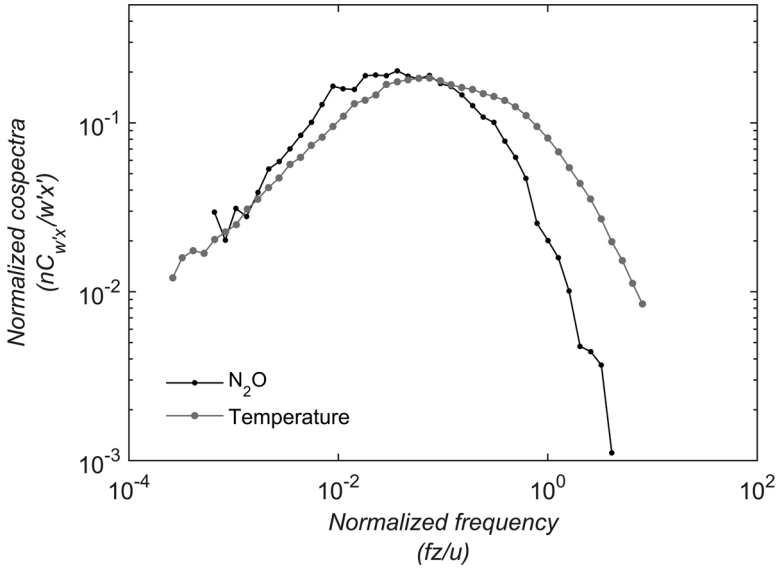

Fig. 1. Normalized cospectral density of temperature and N_2O (f: frequency, z: height, u: wind velocity).

Table 2
Quality criteria for selecting power spectra and performing spectral correction.

	Friction velocity ($m\ s^{-1}$)	Sensible heat flux ($W\ m^{-2}$)	Latent heat flux ($W\ m^{-2}$)	N_2O flux ($nmol\ m^{-2}\ s^{-1}$)
Minimum, unstable	0.2	20	20	1
Minimum, stable	0.05	5	3	0.5
Maximum (stable and unstable)	5	1000	1000	200

several hours to readjust. Therefore, data following a restart (up to 12 h) were also discarded.

The quality of time series was controlled using statistical tests as detailed in Vickers and Mahrt (1997). Settings for CO_2 served as the main basis for N_2O settings and were adapted to best suit the control of N_2O time series quality (see Table S1 in Supplement). The tuning of said parameters was mainly guided by visual examination of time series and with the intent to avoid systematic flagging of behaviors linked to physical events captured by the QCL.

Adequate conditions of stationarity and turbulence were assessed following the tests by Foken and Wichura (1996) with quality classes (Mauder and Foken, 2006); data categorized as level 2 were discarded.

All tests and criteria combined, a total of 29% of N_2O fluxes were discarded. Out of the 8082 half-hours left, 7 were identified as outliers and removed; these fluxes exceeded the weekly median by two to three orders of magnitude.

2.4.2. Influence of friction velocity

Eddy covariance flux data can show sensitivity to friction velocity (u*) which can come from an artifact rather than from actual mechanisms responsible for producing or absorbing the gas of interest (Aubinet et al., 2012). In the case of N_2O, known producing or absorbing mechanisms are not known to be directly influenced by u* and we would expect decreasing fluxes with decreasing u* to be artifact-related.

Assessing the u* threshold under which fluxes are underestimated is usually done by the visualization of temperature-normalized fluxes against u* and the identification of the limit of a plateau at low u* (Aubinet et al., 2012). However, we did not follow this approach with our N_2O measurements: after selecting a range of data less likely to be influenced by fertilizer (4 months after N application) or by precipitation (low soil water content), it was not possible to retrieve a robust relationship between temperature and N_2O fluxes to normalize the latter. Therefore, the u* threshold was instead determined based on CO_2 fluxes measured at the experimental site. First, Eq. (1) was fitted to CO_2 night fluxes (R_{meas}) using the air temperature (T_{air}) as predictor (with R_{10}: ecosystem base respiration at 10 °C, and Q_{10}: temperature sensitivity parameter). Night fluxes were then normalized (R_{norm}) by means of Eq. (2):

$$R_{fit,10} = R_{10} * Q_{10}^{(T_{air}-10)/10} \quad (1)$$

$$R_{norm} = \frac{R_{meas}}{R_{fit,10}} \quad (2)$$

After plotting R_{norm} by classes of friction velocity, it was visually assessed that the u* threshold fell between 0.05 and 0.1 $m\ s^{-1}$ (Fig. 2). This range is very similar to that which Moureaux et al. (2006) found at the same experimental site for a previous sugar beet crop in 2004. The uncertainty related to u* filtering is discussed in Section 2.6.

After applying the u* filter (0.1 $m\ s^{-1}$), 65% of the dataset remained for the analyses (*i.e.* an average of 31 flux measurements per day).

2.5. Data treatment and analyses

2.5.1. Gap-filling

Data gaps were filled at the daily-scale according to the following approach (Mishurov and Kiely, 2011):

(Case 1) If less than 18 half-hours were missing for a day, the daily mean was calculated based on the 30-min fluxes available for that day;

(Case 2) For days missing more than 18 half-hours, daily means were assessed with a moving average using a 7-day rectangular window.

The threshold of 18 missing half-hours was chosen based on 1000 random samplings of [48–N] half-hours out of a complete day. The average daily mean and the associated confidence interval were computed for N varying from 0 to 47. For N under 18, we considered that the gain of confidence in the daily mean weighted by the number of available half-hours did not substantially improve. Therefore, N = 18 represents a suitable trade-off between representativity and data availability. Days missing less than 18 half-hours represented 88% of the dataset.

Two gaps longer than a day occurred in the dataset (July 20–25 and

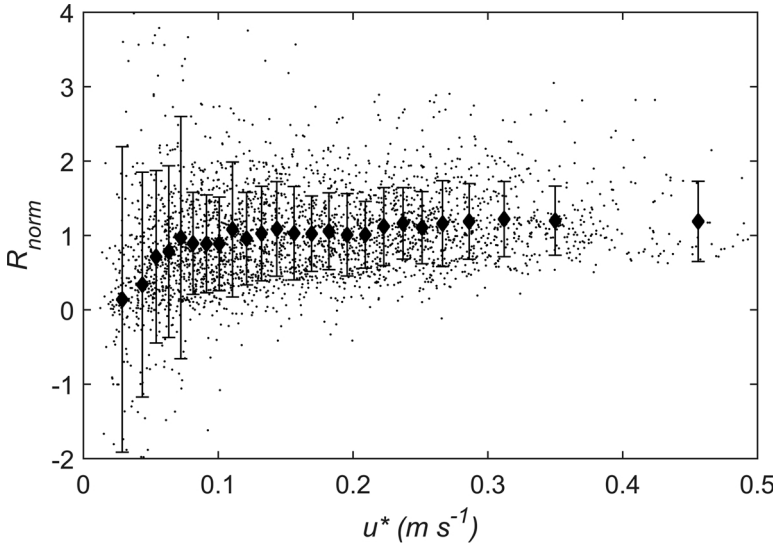

Fig. 2. Normalized CO_2 night fluxes (R_{norm}) by equal-sized classes of friction velocity (u*).

November 1–4). Missing days were replaced by the mean of three days before and three days after the gap (*Case 3*). We assumed that this method did not introduce substantial bias into the budget as both gaps occurred during periods of low and constant fluxes. Enlarging the periods to take into account up to a week of data to fill such gaps did not change its value by more than 5%.

The uncertainty related to gap-filling is discussed in Section 2.6.

2.5.2. N_2O budget

The N_2O budget (or Net Ecosystem Exchange of N_2O, NEE_{N2O}) of the sugar beet crop was calculated based on the gap-filled dataset as the sum of daily fluxes from fertilization to harvest. The crop emission factor was calculated as described in the Tier 1 equation of the IPCC guidelines (De Klein et al., 2006), by dividing the amount of N emitted as N_2O by the amount of N supplied, including fertilizer and crop residues (mineralized nitrogen from land-use change and management was considered negligible). N-amount from crop residues was determined as the yield of buried dry biomass from the previous crop (mustard leaves, stems and roots, and sparse wheat regrowth) multiplied by the estimated content of potentially mobilized N in the previous year (Destain et al., 2010).

NEE_{N2O} was converted to CO_2-equivalent ($NEE_{N2O,\ CO2\text{-}eq}$) by multiplying it by 298, which represents the global warming potential of N_2O over 100 years (Myhre et al., 2013).

2.5.3. Management and meteorological controls of N_2O flux

Daily N_2O fluxes were averaged by class of SWC-5 (< 25%, 25–30%, 30–35%, > 35%) and compared by means of a one-way ANOVA. A one-way ANOVA test was also performed on fluxes averaged over 7 days preceding and 7 days following seed-bed preparation and sowing.

To investigate half-hourly N_2O flux dynamics, fluxes were compared to several temperature dynamics (air, surface, and soil) as temperature is known for its daily cyclic variation. Two contrasting periods were examined: the first emission peak from March 25 to April 12, and a period of background fluxes (daily average < 0.5 nmol m^{-2} s^{-1}) with dry soil from mid-August to mid-September. For each period of interest, half-hourly data (x_i) were standardized with regard to the daily mean ($\bar{x}_d$) and daily standard deviation (s_d) following Eq. (3). Then standardized variables ($x_{stand,i}$) were averaged by time of day, resulting in 48 values per period. Such analyses were performed on non-gap-filled data.

$$x_{stand,i} = \frac{x_i - \bar{x}_d}{s_d} \quad (3)$$

To further analyze the episodes of emission peaks, a linear regression model was fit to daily averaged N_2O fluxes to evaluate a potential correlation with daily averaged CO_2 fluxes (Lognoul et al., 2017).

All statistical analyses were made using Matlab Statistics Toolbox: Matlab Version 2015a (MathWorks, Natrick, MA, USA).

2.6. Evaluation of uncertainties

The total random uncertainty of individual 30-minute fluxes (ε_{30min}) was assessed as proposed by Langford et al. (2015) by calculating the root mean squared deviation from zero in a region of the covariance function far away from the true time-lag (150–200 s). The total random uncertainty was integrated over a day and over the crop season (ε_{season}) following the rules of error propagation (Taylor, 1989), assuming that errors were independent from one period to another (Eqs. (4) and (5)).

$$\varepsilon_{day} = \sqrt{\sum_{i=1}^{48} (\varepsilon_{30min,i})^2} \quad (4)$$

$$\varepsilon_{season} = \sqrt{\sum_{j=1}^{219} (\varepsilon_{day,j})^2} \quad (5)$$

When multiplied by 1.96, the individual random error provides an estimate of the measurement precision at the 95% confidence intervals, which can be used as individual N_2O flux limits of detection, or LOD (Langford et al., 2015).

The budget over the crop season is also subject to other uncertainties. In the case of our dataset, three potential sources were identified: (1) spectral correction, (2) u* filtering, and (3) gap-filling.

The uncertainty related to the spectral correction (δ_{SC}) was approximated *via* the 99%-confidence interval of the regression between SCF and wind speed used to correct half-hourly fluxes.

The uncertainty inherent to u* filtering (δ_{UF}) was approximated by the variation of the non-gap-filled budget over the whole campaign after filtering N_2O fluxes within the plausible range for the u* threshold (from 0.05 to 0.1 m s^{-1}).

The uncertainty related to gap-filling (δ_{GF}) was calculated depending on the number of missing half-hours in a day (SD: standard deviation, 1.96: normal score used to estimate the 95% confidence intervals).

(Case 1) If less than 18 half-hours were missing, the uncertainty of the daily flux was calculated as 1.96*SD of the daily mean;

(Case 2) If more than 18 half-hours were missing, the uncertainty of the daily flux was calculated as 1.96*SD of the moving average;
(Case 3) During the two longer gaps, the uncertainty of the daily mean was calculated as 1.96*SD of the 3 days preceding and 3 days following the gap.

We assumed that between days, errors were random and independent, and we combined the three gap-filling cases to obtain the overall gap-filling uncertainty.

Finally, the four sources of uncertainty (total random uncertainty, spectral correction, u* filtering, and gap-filling) were combined assuming their non-correlation between one another at an annual scale (Eq. (6)– Taylor, 1989).

$$\delta_{total} = \sqrt{(\varepsilon_{season})^2 + (\delta_{SC})^2 + (\delta_{UF})^2 + (\delta_{GF})^2} \quad (6)$$

3. Results

3.1. Ancillary measurements

The evolution of pedo-climatic variables is presented in Fig. 3. The daily soil temperature varied between 5 and 22 °C during the crop season, with warmest temperatures reached in the months of June, July, and August (Fig. 3a).

Cumulative rainfall between March and October 2016 was 454 mm, keeping the global soil water content (SWC) between 20 and 44%. Before fertilization (March 22), the soil water content in all three soil layers (5, 15, and 25 cm) was around 35% (Fig. 3b). Precipitation started 3 days after fertilization, immediately followed by an increase in SWC (reaching about 40%). The rainy weather lasted until the end of April with a weekly average of 14 mm. The soil water content at 5 cm (SWC-5) remained above 32%. The first weeks of May were much drier with SWC-5 decreasing to 25%. Besides a rainy month of June, fewer precipitation events were observed during the summer, followed by a gradual drying of the soil (SWC-5 at its lowest of the cropping season) until mid-October when rainfall resumed. When compared to data collected by the Royal Meteorological Institute of Belgium between the years 1981 and 2010, precipitation at the experimental site in 2016 fell within the Belgian average range (Fig. 4), except a rainy month of June (+66%) and a drier period between August and November (–57%). Note that the month of May was not particularly drier than average but precipitation events were distributed towards the end of the month (Fig. 3b).

The leaf area index of sugar beet is shown in Fig. 3c. After a slight increase in the first two months after sowing, the LAI increased to 3.93 $m^2_{leaf}m^{-2}_{soil}$ to then decrease by 30% until the harvest date. The observed development curve is typical for sugar beet (Theurer, 1979).

3.2. N_2O fluxes

3.2.1. Cumulated N_2O fluxes

The evolution of CO_2 fluxes, N_2O fluxes, and cumulated N_2O emissions are presented in Fig. 5. Fluxes throughout the crop season fluctuated between – 0.81 nmol m^2 s^{-1} and 5.56 nmol m^2 s^{-1}, with an average of 0.34 nmol m^2 s^{-1}. The total amount of N_2O emitted by the sugar beet crop between fertilization and harvest was 6520 µmol N_2O m^{-2}, corresponding to 1.83 kg N_2O-N ha^{-1}. With regard to the N inputs (as fertilizer and crop residues), the sugar beet crop is characterized by an emission factor of 1.2%. We compared this result to various studies including non-cereal crops, rotations, and managed grasslands (Table 3). Our sugar beet crop had a higher EF_1 than other sites fertilized with similar amounts of inorganic N and was one of the few presenting an EF_1 higher than 1% (Fig. 6).

The NEE_{N2O} converted to CO_2-eq was 230 kg CO_2-C m^{-2}. CH_4 was assumed to be negligible in our experiment: the experimental field is located on soil with good drainage, therefore excluding situations of continuous waterlogging that are favorable to methane production (Smith et al., 2003).

3.2.2. Farming and meteorological controls of N_2O fluxes

N_2O exchanges showed high temporal variability: three episodes of intense emission peaks were observed (from March 25 to April 12, from April 30 to May 4, and from May 28 to June 17) and, in between, N_2O fluxes stayed at a background level which hovered around 0.20 nmol m^2 s^{-1}. Over the whole dataset, daily emissions were significantly higher for SWC-5 above 35% (Fig. 7) although rainfall did not systematically trigger emission bursts.

The first emission peak started after fertilization, almost simultaneous with heavy rainfall causing the SWC-5 cm to increase to 40%. This episode lasted until the day of seed bed preparation and sugar beet sowing in the parcel. Immediately after, the emission intensity significantly went down ($p < 0.001$), being reduced by 70% to return to background levels (Fig. 8). Almost a third of the N_2O emitted during the

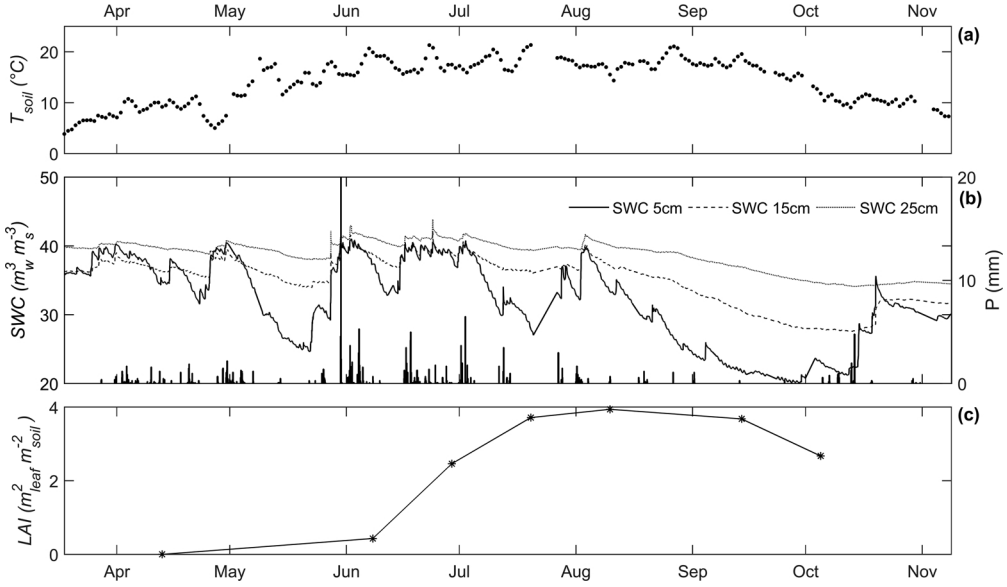

Fig. 3. Evolution of (a) daily averaged soil temperature, (b) 30 min soil water content at 5, 15, and 25 cm, and 30 min precipitation, and (c) leaf area index.

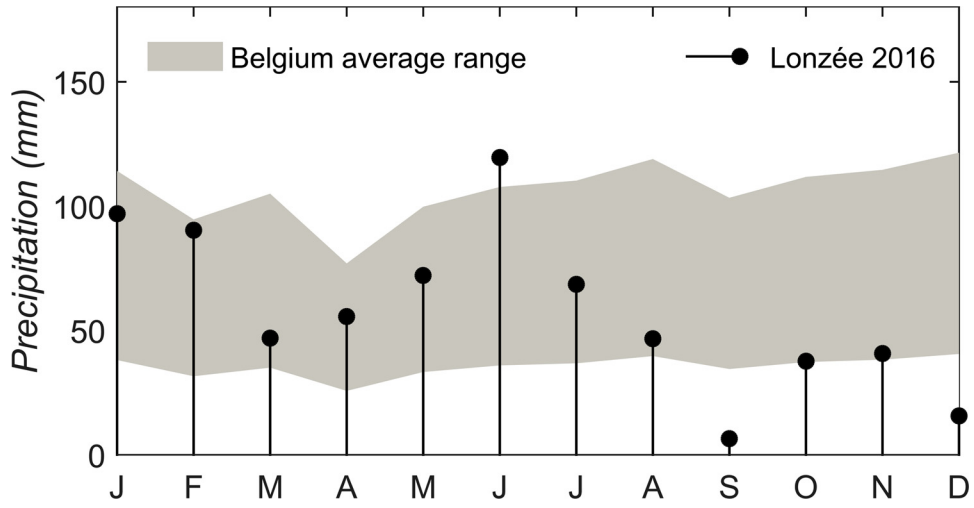

Fig. 4. Belgian average precipitation range between 1981 and 2010 (upper and lower limits: average ± 1*standard deviation) and monthly precipitation at Lonzée ICOS Station in 2016.

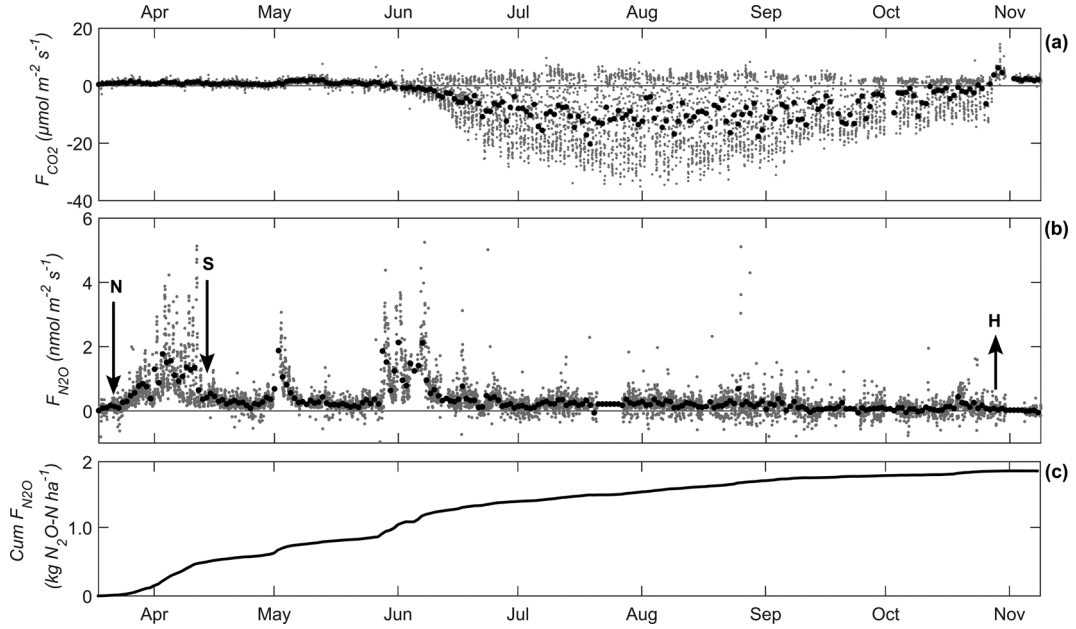

Fig. 5. Evolution of (a) CO_2 fluxes (grey: half-hourly flux, black: daily averaged flux), (b) N_2O fluxes (grey: half-hourly flux, black: daily averaged flux), and (c) cumulated N_2O fluxes. The arrows indicate the farming practices (N: fertilization on March 22, S: soil preparation and sowing on April 12–13, H: harvest on October 27).

whole crop season was exchanged during this peak episode (Fig. 5c). During this first peak, daily N_2O fluxes were significantly correlated to CO_2 fluxes (Fig. 9). No similar significant relation was found for further peak episodes in the dataset or for background fluxes.

A second peak started between April 30 – 17:00 and May 2 – 10:00 (about two days of missing data), at least five days after precipitation and the sudden rise of SWC-5. The burst lasted for 4–5 days. By this time, the SWC-5 had decreased to 34%.

The third N_2O peak episode began on May 28 – 10:00 (more than two months after fertilization), about 15 h after a rainstorm (more than 25 mm of water fell in an hour). Precipitation events went on for a week and were interrupted for a few days (SWC-5 decreased below 35%). It then started to rain again almost every day until the beginning of July. The period that followed was characterized by background N_2O fluxes that lasted until harvest without any noticeable emission burst.

The characteristics of the three peak episodes are summarized in Table 4.

3.2.3. Daily variations in N_2O fluxes

Daily oscillations in N_2O fluxes can be seen, especially between March and July, with daytime fluxes up to 20 times larger than nighttime fluxes. This observation was examined in more detail during two specific periods: one with high emission (first peak from March 25 to April 12) and one with low emission (background flux period from mid-August to mid-September).

During the first N_2O emission peak (March-April), the N_2O fluxes showed a clear daily oscillation with a maximum reached in early afternoon and minimum values during the night (Fig. 10a). This oscillation was better in phase with the surface temperature (T_{surf}) than with T_{air} – although with a slight delay between 09:00 and 12:00 – and the two normalized variables were well correlated ($R^2 = 0.92$, p-value < 0.001). It was not in phase with T_{soil} at 5 cm, with an offset of 2–3 h.

The N_2O diel cycle was less smooth and its amplitude of variation was smaller during the background period than during peaks (Fig. 10b). However, normalized night fluxes were still significantly lower than

Table 3
Emitted N_2O (kg N ha^{-1}), N inputs (kg N ha^{-1}) and associate emission factor (%) from several studies including crops, grassland conversion to crop and mowed grassland.

Study	Measurement method (temporal resolution)	Type of crop (measurement period)	Type of fertilizer	Emitted N_2O	N inputs	EF
Present study[a]	EC (30 min)	Sugar beet (219 d)	Inorganic fertilizer	1.83	160	1.2 (± 0.1)
Merbold et al., 2014[a,b]	EC (30 min)	Restored grassland (365 d)	Manure and inorganic fertilizer	29.10	198	14.71
Fuchs et al., 2018[c]	EC (10 min)	Mowed grassland – year 1 (365 d)	Cattle and pig liquid slurry	4.1	296	1.39
		Mowed grassland – year 2 (365 d)		6.3	181	3.48
Koga, 2013[c]	SCh (10 days)	Sugar beet (156 d)	Inorganic fertilizer	0.18	150	0.12
Seidel et al., 2017	SCh (2 – 7 days)	Perennial grassland – min (300 d)	Various types of cattle slurry	0.40	*572*	0.07
		Perennial grassland – max (300 d)		4.20	*560*	0.75
Pugesgaard et al., 2017	SCh (2 – 4 weeks)	Rotation mean – barley, faba bean, potato, wheat (347 d)	Inorganic fertilizer	0.90	168	0.54
Reinsch et al., 2018[c]	SCh (1 week)	Permanent grassland (365 d)	Cattle slurry	0.65	240	0.27
	SCh (1 week)	Glassland conversion to maize (365 d)	Cattle slurry	1.78	240	0.74
Flechard et al., 2005[c]	ACh (2 hours)	Managed grassland (365 d)	Cattle slurry and inorganic fertilizer	0.2	185	0.6
Laville et al., 2011[a]	ACh (1.5 hour)	Maize (365 d)	Cattle slurry and inorganic fertilizer	2.90	*153*	1.90

EC: eddy covariance. SCh : manual static closed chambers. ACh : automated closed chambers. Italics: value deduced from the two other columns when not provided.
[a] Nitrogen from land use change and management was not included or deemed negligible.
[b] Not included in the associated graph (Fig. 6).
[c] The factor was determined by comparing a treated plot and a control plot.

day fluxes (p-value < 0.01). The daily cycle seemed in phase with the air temperature and was better correlated with this variable (R^2 = 0.33, p-value < 0.001) than with T_{soil} at 5 cm and with $T_{surface}$ (note that, by this time of the year, the surface temperature was considered to be the sugar beet canopy temperature).

3.3. Evaluation of uncertainties

The absolute total random error (ε_{season}) over the crop season was 5 g N_2O-N ha^{-1}. This corresponds to a relative error of 0.3%, whereas the relative error at the 30 min scale ranged from 2 to 850%, with an average of 30% (20% during unstable conditions and 60% during stable conditions). 23% of N_2O fluxes lay under their respective LOD. However, these were not excluded from our dataset as doing so might induce a bias in flux averages over longer periods (Langford et al., 2015). The absolute and total random errors on individual 30 min fluxes, as well as LOD are illustrated in Fig. 11. Negative fluxes were observed during the whole measurement campaign. Such fluxes could be seen as biophysically implausible in our experimental site (Chapuis-Lardy et al., 2007) and most of them were inferior to their LOD. However, they were also not discarded to avoid a systematic bias.

The uncertainty from spectral correction of the N_2O budget over the whole campaign was 52 g N_2O-N ha^{-1} (relative uncertainty: 2.8%). On average, the relative uncertainties for unstable and stable conditions were respectively 1.4% and 3.9%.

Regarding u* filtering, an absolute uncertainty of 149 g N_2O-N ha^{-1} (relative uncertainty: 8.2%) for the N_2O budget was found for the u* threshold range (from 0.05 to 0.1 m s^{-1}).

Regarding gap-filling, the three gap cases (Cases 1, 2, and 3) combined resulted in an overall uncertainty of 148 g N_2O-N ha^{-1} (8.1%), after considering this, between days errors were random and independent. We noted that the absolute uncertainty of daily means during long gaps in background fluxes (0.20 nmol $m^{-2}s^{-1}$) was 6 times smaller than the uncertainty for a one-day gap on May 1 during the second emission peak (1.29 nmol $m^{-2}s^{-1}$). The relative uncertainty during the background emissions was smaller as well (96% and 190% for background and peak respectively).

The total uncertainty of the N_2O budget reached 217 g N_2O-N ha^{-1} (12%). The absolute and relative uncertainties are summarized in Table 5.

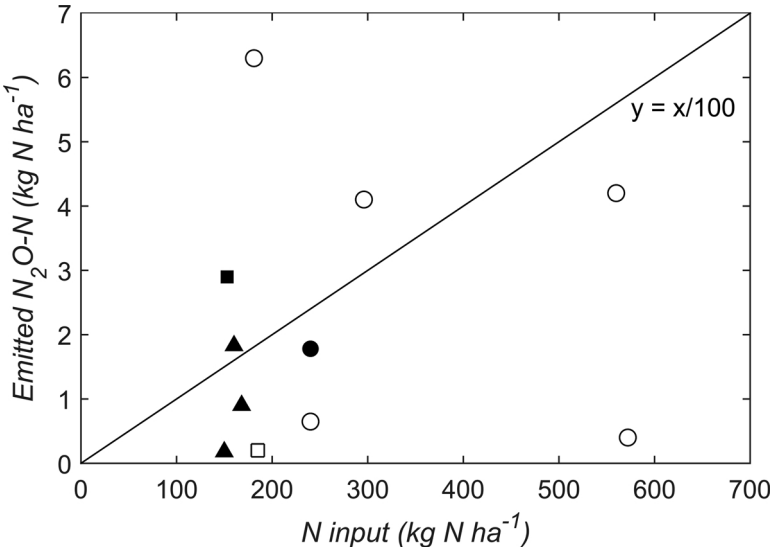

Fig. 6. Comparison of emission factors from studies featuring different types of fertilizer (circles: organic fertilizer, triangle: inorganic fertilizer, square: both) and types of vegetation (filled: crop and grassland conversion to crop, empty: managed grassland). The diagonal line represents an emission factor (EF) of 1%. Exact values and references for each study are given in Table 3.

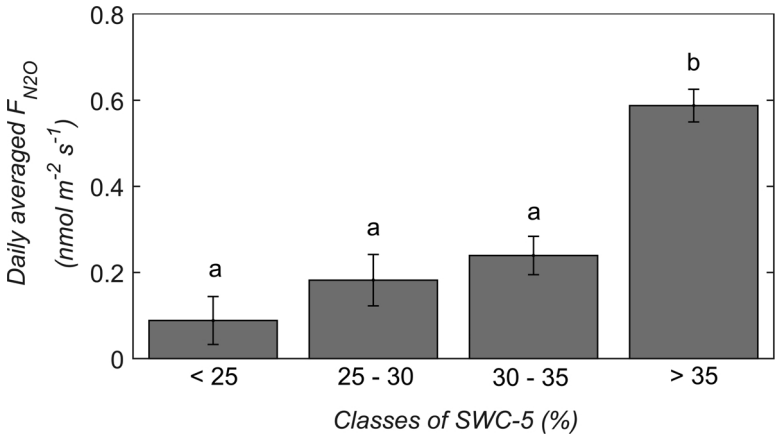

Fig. 7. Daily averaged N_2O flux by classes of soil water content at 5 cm (SWC-5). Different letters over bars indicate a significant difference ($p < 0.001$).

4. Discussion

4.1. Dynamics of N_2O fluxes

4.1.1. Short-term effects of farming practice

Three episodes of high N_2O emissions were observed over the crop season. They were characterized by different durations and flux variations (Table 4), illustrating the great variability of N_2O emissions (Molodovskaya et al., 2012).

The first peak episode was triggered within hours by heavy precipitation following N application. Such a rapid increase of water content and N availability in the soil is well-known to favor N_2O production by micro-organisms (Butterbach-Bahl et al., 2013; Plaza-Bonilla et al., 2014), and during the whole measurement period, N_2O emissions were on average higher for SWC-5 greater than 35% (Fig. 7). It was, however, impossible to identify the production mechanism responsible for the high fluxes. Although high soil water contents are usually associated with denitrification (Linn and Doran, 1984; Dobbie et al., 1999; Bateman and Baggs, 2005), a recent study, conducted under soil and climate conditions similar to our study, found that N_2O emissions were positively correlated to nitrification gene transcripts despite an elevated water-filled pore space (Theodorakopoulos et al., 2017). Meanwhile, when looking at soil temperatures during that peak episode, nitrification could be thought to prevail: while nitrifiers are still active above 5 °C, denitrification rates are usually low below 15 °C (Bouwman, 1990).

Seed-bed preparation and sowing were performed 18 days after the first peak started, consequently reducing N_2O fluxes for two weeks. Although the SWC had decreased, it returned to previous levels within that period without N_2O fluxes rising again (Fig. 8). The soil temperature remained stable (around 10 °C) for 12 days after sowing. These two observations suggest that soil disturbance was the sole cause of this inhibition. To our knowledge, such immediate impact of soil disturbance has not yet been observed.

The influence of tillage in the long term has already been studied without an emerging consensus. On one hand, some have measured enhanced emissions under reduced or no tillage in comparison with conventional tillage, attributing their observations to poorer soil

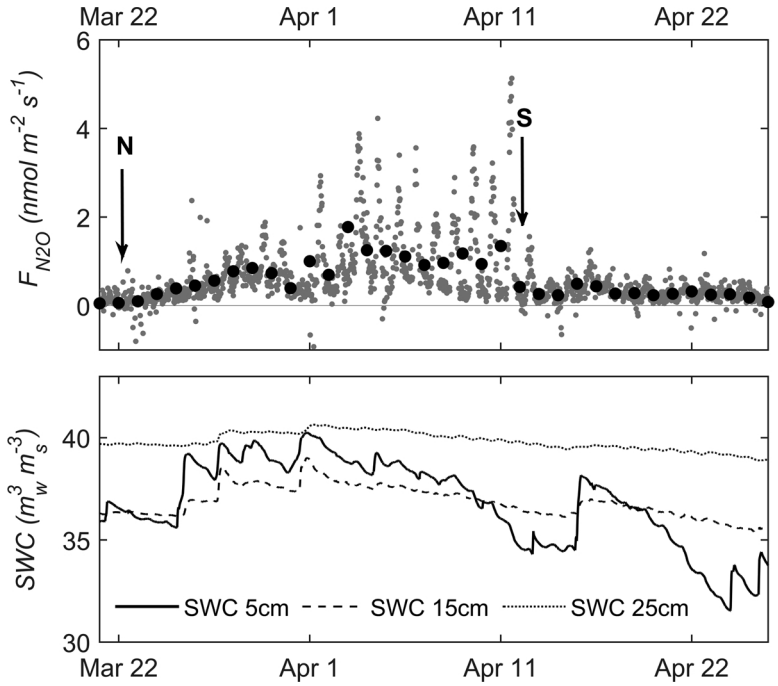

Fig. 8. Focus on the soil preparation and sowing event. Top: N_2O fluxes (grey: 30 min flux, black: daily averaged flux). Bottom: 30 min SWC at 5 (plain line), 15 (dashed line), and 25 cm (dotted line).

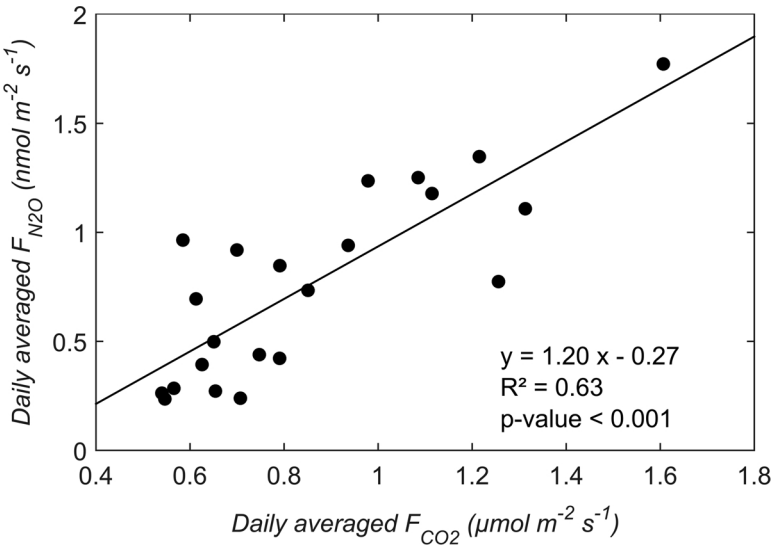

Fig. 9. Correlation between daily averaged CO_2 flux and N_2O flux during the first episode of peak emissions.

aeration promoting denitrification (Mutegi et al., 2010) or to crop residues left near the soil surface (Lognoul et al., 2017). On the other hand, others have attributed greater N_2O emissions to ploughed fields: such practice would promote microbial N_2O production in the long term by incorporating manure and residues into soil aggregates (Koga, 2013). The short-term effect of soil disturbance is rarely investigated, mostly because of a lack of sufficient temporal resolution or because tillage practice and fertilization are performed at the same time (Žurovec et al., 2017). Soil perturbation has been shown to enhance N_2O emission in the medium term (Žurovec et al., 2017). Ebrahimi and Or (2016) modelled N_2O-related activities in soil to find that anaerobic activity was favored in large aggregates. It could be inferred that soil disturbance inhibits denitrification (and therefore emissions), by breaking up bulks and leading to aerobic conditions. However, we cannot confirm that the peak resulted solely from denitrification and this hypothesis alone cannot explain why the second peak episode started 5 days after the last rainfall, while the third one followed the last rainfall by only 15 h.

The delay between rainfall and the second peak episode suggests that the microbial community took some time to build back up after being disturbed by seed-bed preparation. The soil temperature decreased during that associated rain event but stayed high enough for nitrifiers to be active, and remained mostly similar to the temperatures observed in the beginning of the first high emission episode. We thus hypothesized that the microbiome producing N_2O was active at the very surface of the soil before either being shut down by disturbed surface conditions or being relocated deeper. More research is needed to verify this hypothesis since the reactivity to perturbations of N_2O producers in aggregates and the related regulating factors have not yet been studied (Wang et al., 2018).

A third of the total N_2O produced by the crop was emitted between fertilization and seed-bed preparation, and the inhibiting effect observed immediately after sowing was attributed to soil disturbance. Further research on mitigation strategies should thus investigate the impact of the timing between such farming operations.

We excluded the predominance of abiotically produced N_2O at the soil surface as during the first peak episode daily N_2O fluxes were significantly correlated to CO_2 fluxes (Fig. 9), which represent soil respiration at this stage of the crop season. This correlation hints at a significant role of microbial activity following fertilization. The emergence of sugar beet photosynthetic organs reversing CO_2 net exchange explains the absence of correlation during the other two episodes of high flux.

The last peak episode occurred two months after fertilization. Comparable late bursts have been observed under similar soil and climate conditions, which were attributed to crop residue mineralization (Lognoul et al., 2017). Although mustard residues were incorporated prior to the sugar beet crop, it cannot be excluded that this peak originated from remaining N fertilizer rather than solely from mineralization. Sugar beet usually absorbs less than 15% of its nitrogen requirements in April and May (Legrand and Vanstallen, 2000), which corresponds to seed germination and emergence (Didier, 2013). N content can thus remain high until three months after fertilization under such conditions of crop type, climate, and soil texture (Lenz, 2007).

4.1.2. Daily variation of N_2O fluxes

Day fluxes were higher than night fluxes throughout the whole

Table 4
Summarized specificities of episodes of N_2O burst during the crop season.

Specificities	First episode	Second episode	**Third episode**
Start date	March 25	April 30	May 28
Duration	18 d	5 d	21 d
Time after fertilization	3 d	39 d	67 d
Time after last rainfall	1 h	5 d	15 h
Average SWC_5	38.3 %	38.4 %	37.7 %
Average T_{air}	15.0 °C	15.8 °C	21.4 °C
Average daytime flux	1.26 nmol m^{-2} s^{-1}	1.10 nmol m^{-2} s^{-1}	0.90 nmol m^{-2} s^{-1}
Average nighttime flux	0.59 nmol m^{-2} s^{-1}	0.87 nmol m^{-2} s^{-1}	0.71 nmol m^{-2} s^{-1}
Part in total emissions over the measurement campaign	28 %	7 %	24 %
Correlation with CO_2	***	NS	NS

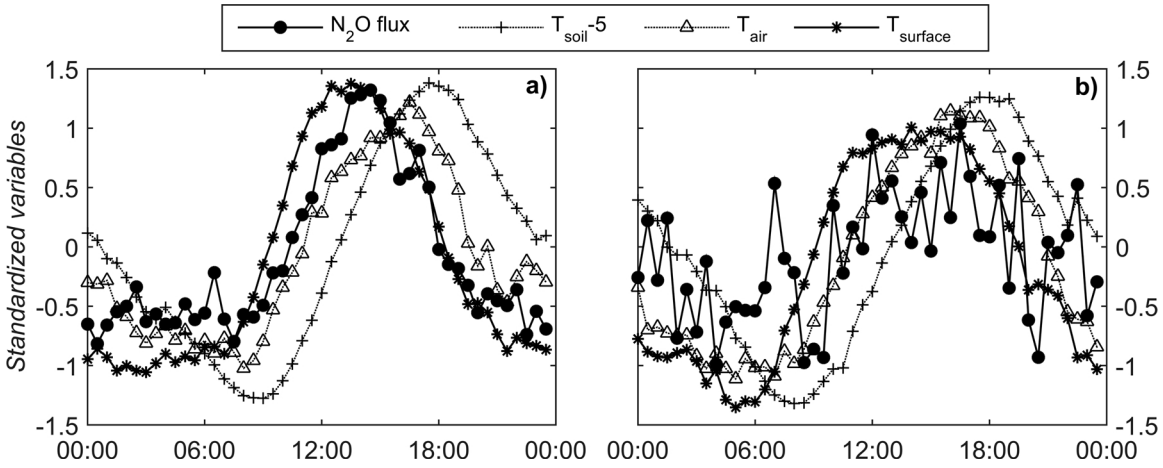

Fig. 10. Daily averaged variation of standardized N_2O fluxes (circles), surface temperature (stars), air temperature (triangles) and soil temperature at 5 cm depth (crosses) during (a) the first N_2O burst episode (March 25 to April 12) and during (b) the background emission period in the summer (August 15 to September 20).

experiment and a diel pattern was clearly identified during peak episodes (Fig. 10a). These observations align with the known control of temperature on N_2O-related microbial activity (Smith et al., 2003). Moreover, intense microbial activity during the day can further decrease O_2 availability in soil pores, acting as a positive feedback on anaerobic production of N_2O by denitrifiers when nitrate substrates are available (Flechard et al., 2007). This would mean that denitrification could be stimulated in conditions of hot and dry weather, with anaerobic zones extending without being necessarily due to precipitation. Denitrification could thus have played a significant role in the higher day emissions observed during the background flux period (Fig. 10b).

The diel cycle observed during peak episodes was in phase with the surface temperature rather than with deeper temperatures. This supports the assumption issued earlier of a N_2O-producing microbial community located in the topmost soil layer. Similar observations were made by Laville et al. (2011) for a fertilized crop over a period of 9 days, while others found a correlation with deeper temperatures (Alves et al., 2012; Livesley et al., 2008). Keane et al. (2017) observed a

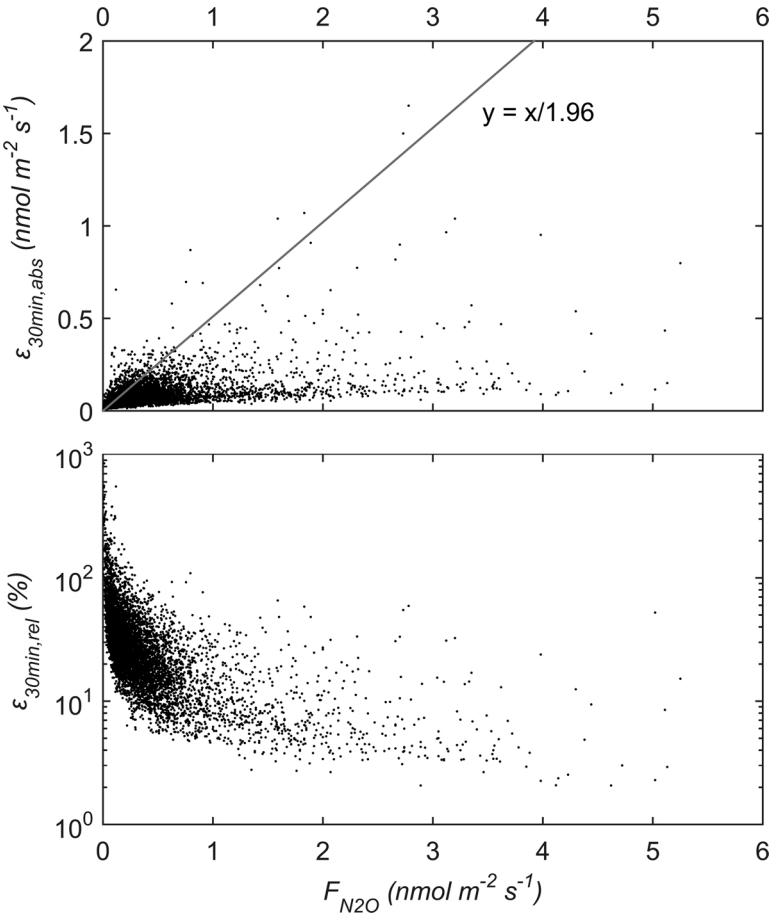

Fig. 11. Total random uncertainty of absolute 30 min N_2O fluxes (top: absolute uncertainty, bottom: relative uncertainty). Observations lying above the line fall under their individual limit of detection ($LOD_{30min} = 1.96*\varepsilon_{30min}$).

Table 5
- Summarized uncertainties of the N_2O budget over the whole crop season.

Source of uncertainty	Absolute uncertainty (g N_2O-N ha^{-1})	Relative uncertainty (%)
Total random error (ε_{season})	5	0.3
Spectral correction (δ_{SC})	52	2.8
u* filtering (δ_{UF})	149	8.2
Gap-filling (δ_{GF})	148	8.1
Total uncertainty (δ_{tot})	217	12

similar correlation but their interpretation of this as an effect of photosynthetically active radiation mediating exuded photosynthetate-C in the root zone, favoring microbial mechanisms producing N_2O (Van Zwieten et al., 2013) doesn't hold in the present case as sugar beet had still not emerged. The hypothesis of a prevailing effect of temperature on microorganisms is thus retained for the first months of our experiment.

The daily pattern observed during the second and third peak episodes was less obvious (Table 4). On one hand, we observed larger night emissions than during the first peak episode, which could originate from a higher range of temperatures in May and June promoting nightly microbial activity. On the other hand, day fluxes were smaller than in April: day emission potential could be dampened by reduced N availability over time. Although direct measurements of soil N content were not available for the present study, N availability should be taken into account along with soil temperatures when explaining N_2O flux variability, as these are poor predictors if considered separately (Lai and Denton, 2017).

Our results highlight that when studying N_2O flux dynamics, several time-scales can be considered. Increases in soil water content near the surface (5 cm depth), in combination with active microorganisms and sufficient N availability, can trigger large emission episodes during the cropping season (immediately or with delay), while the surface temperature drives daily variations in N_2O emissions.

4.2. Cumulated N_2O emissions

A total of 1.83 (± 0.21) kg N_2O-N ha^{-1} was lost through N_2O emissions between the fertilization of the sugar beet crop (March 2016) and its harvest (October 2016). This corresponds to an emission factor (EF_1) of 1.2%, which is slightly larger than the annual estimate of 1% given by the IPCC guidelines (De Klein et al., 2006) used in Belgium. We believe that our EF_1 could have been even higher if the whole year had been monitored: emissions during bare soil periods, although presumed to be low, could have been added to the N_2O budget. In addition, more N_2O emissions could have been expected if the month of May had not been as dry for the most part. Higher soil water content would have promoted higher N_2O emissions, as at that time N availability in the soil was not yet limiting. The EF_1 of our crop was higher than other sites fertilized with similar amounts of inorganic N, and was one of the few presenting an EF_1 higher than 1% (Fig. 6). Given the variety of results that can be obtained with different types of fertilizers and crops, a refinement of emission factor estimates is needed to take farming specificities into account when assessing N_2O emissions. However, our comparison is to be taken with caution, as studies monitoring N_2O fluxes at a sub-daily temporal resolution (using eddy covariance or automatic chambers) tended to give significantly higher EF that the others. It is not excluded that lower EF_1 values originate from (1) a lack of observations late after fertilization (Lognoul et al., 2017), or (2) an insufficient temporal resolution leading to missing short peaks similar to the second emission episode observed in this experiment. More measurements at higher temporal resolution are needed to refine the comparison.

Buysse et al. (2017) estimated the Net Biome Production (NBP) of the experimental site over 12 years (*i.e.* three 4 year crop rotations). When including harvest and C importation (manure, slimes), they found that the site was a net source of C with an annual average loss of 820 kg C ha^{-1}. Sleutel et al. (2003) calculated the annual NBP of Belgian cropland in the silt-loam region (based on C stock inventories over 10 years) and found a similar value (NBP = 900 kg C ha^{-1}). A much lower annual estimate was found by Goidts and van Wesemael (2007) for cropland in Southern Belgium from 1955 to 2005 (120 kg C ha^{-1}). After adding the $NEE_{N2O,\ CO2\text{-}eq}$ to these NBP estimates, we found a net greenhouse gas balance (NGB) varying from 350 to 1130 kg C ha^{-1}. Thus N_2O emissions would account for 20% to 66% of the NGB, highlighting the importance of including N_2O when assessing the GHG budget from a fertilized crop.

4.3. Evaluation of uncertainties

Uncertainties in eddy covariance fluxes are not often investigated (Kroon et al., 2010) although such information is important for the purposes of inter-site comparison and accurate estimates of GHG exchanges. In this study, uncertainties were addressed separately depending on the source, to then be combined in the N_2O budget as uncorrelated uncertainties.

The relative total random error of individual eddy fluxes was rather important (up to 850%) which is similar to the findings of Kroon et al. (2010). This error increased with decreasing flux amplitude (Fig. 11), due to larger signal-to-noise ratios in small fluxes (Langford et al., 2015). This error was reduced to less than one percent after integrating N_2O fluxes over several months. Total random error of the budget was thus negligible compared to the other sources of uncertainty.

The uncertainty related to spectral correction was smaller than 3%, most likely because of the good amount of high-quality fluxes used to build the spectral correction regressions (SCF as a function of wind speed). This source of uncertainty was small in comparison to those others linked to data treatment (respectively three and four times larger for u* filtering and gap-filling, Table 5). In future experiments, a reduction of the uncertainty might be achieved by refining data treatment procedures, *e.g.* upgrading the gap-filling technique to a mechanical approach, or narrowing the u* threshold range by using more data.

Regarding gap-filling, our results also highlight the importance of performing continuous measurements during high emissions, as the uncertainty associated with missing data is larger during peaks than during background flux periods. This is due to greater flux variability during high emission bursts, leading to larger confidence intervals on the gap-filling value.

While the total uncertainty of the N_2O budget was estimated at 12% (217 g N2O-N ha^{-1}), it represented less than 3% when considering the NGB at the site. Thus, using eddy covariance to measure N_2O fluxes appears to be a reliable method when it comes to NGB assessment.

5. Conclusion

Our study aimed to assess the short-term response of N_2O fluxes to weather and farming practices in a sugar beet crop. Measurements were performed from fertilization to harvest using the eddy covariance technique, which enabled the recording of a continuous stream of data at a high temporal resolution.

N_2O emissions were characterized by a diel pattern that correlated well with variations of surface temperature. This suggests that microorganisms responsible for N_2O production were active at the very surface of the soil. The activity of those microorganisms was significantly inhibited by seed-bed preparation. This is the first time that a short-term effect of soil disturbance on N_2O flux has been observed in a crop. An important part of the total N_2O-N loss over the crop season occurred between fertilization and seed-bed preparation. The influence of these farming practices should thus be investigated further to implement mitigation strategies. For example, (i) how does the timing between fertilization and seed-bed preparation affect the total N_2O emissions,

and (ii) do N_2O emissions display an inhibited behavior following other tillage practices, such as stubble breaking or ploughing?

To better understand the underlying mechanisms behind the immediate effect of soil disturbance on N_2O emissions, more *in situ* studies are needed measuring N_2O fluxes at high temporal resolution in crops. We also recommend that researchers assess bulk density and mineral N content (ammonium and nitrate) before and after each farming practice to have a better view of the evolution of soil characteristics and how these are affected by soil disturbance. Finally, investigating the real-time activity of nitrifiers and denitrifiers will help to understand the dynamics of N_2O production in soil aggregates.

Acknowledgments

The authors wish to thank Alain Debacq and Alwin Naiken for N_2O set-up installation and station monitoring, the farmer Philippe Van Eyck, and the Lonzée-ICOS team for site follow-up and measurement of environmental parameters. Margaux Lognoul holds a Research Fellow Grant from the FRS-FNRS, Belgium (A215-MCF/DM-A362 FC 95918). This research has also been facilitated by the NO(EC)2 project also funded by the FRS-FNRS.

Appendix A. Supplementary data

Supplementary material related to this article can be found, in the online version, at doi:https://doi.org/10.1016/j.agrformet.2019.02.033.

References

Abdalla, M., Osborne, B., Lanigan, G., Forristal, D., Williams, M., Smith, P., Jones, M.B., 2013. Conservation tillage systems: a review of its consequences for greenhouse gas emissions. Soil Use Manage. 29, 199–209. https://doi.org/10.1111/sum.12030.

Alves, B.J.R., Smith, K.A., Flores, R.A., Cardoso, A.S., Oliveira, W.R.D., Jantalia, C.P., Urquiaga, S., Boddey, R.M., 2012. Selection of the most suitable sampling time for static chambers for the estimation of daily mean N2O flux from soils. Soil Biol. Biochem. 46, 129–135. https://doi.org/10.1016/j.soilbio.2011.11.022.

Aubinet, M., Vesala, T., Papale, D., 2012. Eddy Covariance : A Practical Guide to Measurement and Data Analysis. Springer. ed., New York. https://doi.org/10.1007/978-94-007-2351-1.

Bateman, E.J., Baggs, E.M., 2005. Contributions of nitrification and denitrification to N2O emissions from soils at different water-filled pore space. Biol. Fertil. Soils 41, 379–388. https://doi.org/10.1007/s00374-005-0858-3.

Bouwman, A.F., 1990. Exchange of greenhouse gases between terrestrial ecosystems and the atmosphere. In: Bouwman, A.F. (Ed.), Soils and the Greenhouse Effect. John Wiley and Sons, New York, pp. pp. 61–127.

Bracker, G., Conrad, R., 2011. Diversity, structure, and size of N2O-Producing microbial communities in soils — what matters for their functioning? Adv. Appl. Microbiol. 75, 33–70.

Butterbach-Bahl, K., Baggs, E.M., Dannenmann, M., Kiese, R., Zechmeister-Boltenstern, S., 2013. Nitrous oxide emissions from soils: how well do we understand the processes and their controls? Philos. Trans. R. Soc. Lond. Ser. B Biol. Sci. 368https://doi.org/10.1098/rstb.2013.0122. 20130122.

Buysse, P., Bodson, B., Debacq, A., De Ligne, A., Heinesch, B., Manise, T., Moureaux, C., Aubinet, M., 2017. Carbon budget measurement over 12 years at a crop production site in the silty-loam region in Belgium. Agric. For. Meteorol. 246, 241–255. https://doi.org/10.1016/j.agrformet.2017.07.004.

Castellano, M.J., Schmidt, J.P., Kaye, J.P., Walker, C., Graham, C.B., Lin, H., Dell, C.J., 2010. Hydrological and biogeochemical controls on the timing and magnitude of nitrous oxide flux across an agricultural landscape. Glob. Change Biol. 16, 2711–2720. https://doi.org/10.1111/j.1365-2486.2009.02116.x.

Chapuis-Lardy, L., Wrage, N., Metay, A., Chotte, J.L., Bernoux, M., 2007. Soils, a sink for N2O? A review. Glob. Change Biol. 13, 1–17. https://doi.org/10.1111/j.1365-2486.2006.01280.x.

Ciais, P., Sabine, C., Bala, G., Bopp, L., Brovkin, V., Canadell, J., Chhabra, A., DeFries, R., Galloway, J., Heimann, M., Jones, C., Quéré, C.Le, Myneni, R.B., Piao, S., Thornton, P., 2013. Carbon and other biogeochemical cycles. Climate Change 2013: The Physical Science Basis. Contribution of Working Group I to the Fifth Assessment Report of the Intergovernmental Panel on Climate Change. https://doi.org/10.1017/CBO9781107415324.015.

Conrad, R., 1996. Soil microorganisms as controllers of atmospheric trace gases (H2, CO, CH4, OCS, N2O, and NO). Microbiol. Rev. 60, 609–640. https://doi.org/10.1007/978-3-642-61096-7_11.

D'Haene, K., Van Den Bossche, A., Vandenbruwane, J., De Neve, S., Gabriels, D., Hofman, G., 2008. The effect of reduced tillage on nitrous oxide emissions of silt loam soils. Biol. Fertil. Soils 45, 213–217. https://doi.org/10.1007/s00374-008-0330-2.

De Klein, C., Novoa, R., Ogle, S., Smith, K., Rochette, P., Wirth, T., 2006. Chapter 11: N2O emissions from managed soils, and CO2 emissions from lime and urea application. 2006 IPCC Guidelines for National Greenhouse Gas Inventories.

De Ligne, A., 2018. ICOS Label Report – Lonzée. Belgium. Unpublished data. .

Destain, J.P., Reuter, V., Goffart, J.P., 2010. Autumn cover crops and green manures: environment protection and agronomic interest. Biotechnol. Agron. Soc. Environ. 14, 73–78.

Didier, A., 2013. Modélisation de la croissance, des relations sources-puits et du rendement en sucre de la betterave sucrière (Beta vulgaris L.) sous des régimes contrastés de nutrition azotée. French. Sciences agricoles. AgroParisTech.

Dobbie, K.E., McTaggart, I.P., Smith, Ka., 1999. Nitrous oxide emissions from intensive agricultural systems: variations between crops and seasons, key driving variables, and mean emission factors. J. Geophys. Res. 104, 26891–26899. https://doi.org/10.1029/1999JD900378.

Drury, C.F., Reynolds, W.D., Tan, C.S., Welacky, T.W., Calder, W., McLaughlin, N.B., 2006. Emissions of Nitrous Oxide and Carbon Dioxide: influence of tillage type and nitrogen placement depth. Soil Sci. Soc. Am. J. 70, 570–581. https://doi.org/10.2136/sssaj2005.0042.

Ebrahimi, A., Or, D., 2016. Microbial community dynamics in soil aggregates shape biogeochemical gas fluxes from soil profiles - upscaling an aggregate biophysical model. Glob. Change Biol. 22, 3141–3156. https://doi.org/10.1111/gcb.13345.

Flechard, C.R., Neftel, A., Jocher, M., Ammann, C., Fuhrer, J., 2005. Bi-directional soil/atmosphere N2O exchange over two mown grassland systems with contrasting management practices. Glob. Change Biol. 11, 2114–2127. https://doi.org/10.1111/j.1365-2486.2005.01056.x.

Flechard, C.R., Ambus, P., Skiba, U., Rees, R.M., Hensen, a., van Amstel, a., Dasselaar, a V.D.P.Van, Soussana, J.F., Jones, M., Clifton-Brown, J., Raschi, a., Horvath, L., Neftel, a., Jocher, M., Ammann, C., Leifeld, J., Fuhrer, J., Calanca, P., Thalman, E., Pilegaard, K., Di Marco, C., Campbell, C., Nemitz, E., Hargreaves, K.J., Levy, P.E., Ball, B.C., Jones, S.K., van de Bulk, W.C.M., Groot, T., Blom, M., Domingues, R., Kasper, G., Allard, V., Ceschia, E., Cellier, P., Laville, P., Henault, C., Bizouard, F., Abdalla, M., Williams, M., Baronti, S., Berretti, F., Grosz, B., 2007. Effects of climate and management intensity on nitrous oxide emissions in grassland systems across Europe. Agric. Ecosyst. Environ. 121, 135–152. https://doi.org/10.1016/j.agee.2006.12.024.

Foken, T., Wichura, B., 1996. Tools for quality assessment of surface based flux measurement. Agric. For. Meteorol. 78, 83–105. https://doi.org/10.1016/0168-1923(95)02248-1.

Foken, T., Leuning, R., Oncley, S., Mauder, M., Aubinet, M., 2012. Corrections and data quality control. Eddy Covariance: A Practical Guide to Measurement and Data. Springer. ed., New York, pp. pp. 85–131.

Fratini, G., Ibrom, A., Arriga, N., Burba, G., Papale, D., 2012. Relative humidity effects on water vapour fluxes measured with closed-path eddy-covariance systems with short sampling lines. Agric. For. Meteorol. 165, 53–63. https://doi.org/10.1016/j.agrformet.2012.05.018.

Fuchs, K., Hörtnagl, L., Buchmann, N., Eugster, W., Snow, V., Merbold, L., 2018. Management matters: testing a mitigation strategy for nitrous oxide emissions on intensively managed grassland. Biogeosci. Discuss. 1–43. https://doi.org/10.5194/bg-2018-192.

Goidts, E., van Wesemael, B., 2007. Regional assessment of soil organic carbon changes under agriculture in Southern Belgium (1955-2005). Geoderma 141, 341–354. https://doi.org/10.1016/j.geoderma.2007.06.013.

Groffman, G.P., Robertson, G.P., 2007. Nitrogen transformation. Soil Microbiology, Chemistry, and Ecology 341–364.

Hénault, C., Grossel, a., Mary, B., Roussel, M., LéOnard, J., 2012. Nitrous oxide emission by agricultural soils: a review of spatial and temporal variability for mitigation. Pedosphere 22, 426–433. https://doi.org/10.1016/S1002-0160(12)60029-0.

Horst, T.W., Lenschow, D.H., 2009. Attenuation of scalar fluxes measured with spatially-displaced sensors. Bound.-Layer Meteorol. 130, 275–300. https://doi.org/10.1007/s10546-008-9348-0.

IRCEL (Belgian Interregional Environment Agency), 2017. Belgium's Greenhouse Gas Inventory (1995-2015) - National Inventory Report Submitted Under the United Nations Framework Convention on Climate Change.

Jahangir, M.M.R., Roobroeck, D., van Cleemput, O., Boeckx, P., 2011. Spatial variability and biophysicochemical controls on N2O emissions from differently tilled arable soils. Biol. Fertil. Soils 47, 753–766. https://doi.org/10.1007/s00374-011-0580-2.

Keane, B.J., Ineson, P., Vallack, H.W., Blei, E., Bentley, M., Howarth, S., McNamara, N.P., Rowe, R.L., Williams, M., Toet, S., 2017. Greenhouse gas emissions from the energy crop oilseed rape (Brassica napus); the role of photosynthetically active radiation in diurnal N 2 O flux variation. Glob. Change Biol. Bioenergy. https://doi.org/10.1111/gcbb.12491.

Koga, N., 2013. Nitrous oxide emissions under a four-year crop rotation system in northern Japan: impacts of reduced tillage, composted cattle manure application and increased plant residue input. Soil Sci. Plant Nutr. 59, 56–68. https://doi.org/10.1080/00380768.2012.733870.

Kroon, P.S., Hensen, a., Van Den Bulk, W.C.M., Jongejan, Pa C., Vermeulen, a.T., 2008. The importance of reducing the systematic error due to non-linearity in N2O flux measurements by static chambers. Nutr. Cycl. Agroecosyst. 82, 175–186. https://doi.org/10.1007/s10705-008-9179-x.

Kroon, P.S., Hensen, A., Jonker, H.J.J., Ouwersloot, H.G., Vermeulen, A.T., Bosveld, F.C., 2010. Uncertainties in eddy covariance flux measurements assessed from CH4and N2O observations. Agric. For. Meteorol. 150, 806–816. https://doi.org/10.1016/j.agrformet.2009.08.008.

Lai, T.V., Denton, M.D., 2017. N2O and N2 emissions from denitrification respond differently to temperature and nitrogen supply. J. Soils Sedim. 18, 1–10. https://doi.org/10.1007/s11368-017-1863-5.

Lammirato, C., Lebender, U., Tierling, J., Lammel, J., 2018. Analysis of uncertainty for N2O fluxes measured with the closed-chamber method under field conditions: calculation method, detection limit, and spatial variability. J. Plant Nutr. Soil Sci. 181, 78–89. https://doi.org/10.1002/jpln.201600499.

Langford, B., Acton, W., Ammann, C., Valach, a., Nemitz, E., 2015. Eddy-covariance data with low signal-to-noise ratio: time-lag determination, uncertainties and limit of detection. Atmos. Meas. Tech. Discuss. 8, 2913–2955. https://doi.org/10.5194/amtd-8-2913-2015.

Laudinat, V., 2015. Culture De La Betterave Sucrière. Institut Technique de la Betterave, Paris, France.

Laville, P., Lehuger, S., Loubet, B., Chaumartin, F., Cellier, P., 2011. Effect of management, climate and soil conditions on N2O and NO emissions from an arable crop rotation using high temporal resolution measurements. Agric. For. Meteorol. 151, 228–240. https://doi.org/10.1016/j.agrformet.2010.10.008.

Legrand, G., Vanstallen, M., 2000. Fumure Azotée En Betterave Sucrière - Les Guides Techniques De l'IRBAB. Institut Royal Belge pour l'Amélioration de la Betterave (IRBAB/KBIVB), Tirlemont.

Lenz, V., 2007. A Process-based Crop Growth Model for Assessing Global Change Effects on Biomass Production and Water Demand. University of Cologne.

Linn, D.M., Doran, J.W., 1984. Effect of Water-Filled Pore Space on Carbon Dioxide and Nitrous Oxide Production in Tilled and Nontilled Soils. Soil Sci. Soc. Am. J. 48https://doi.org/10.2136/sssaj1984.03615995004800060013x. 12671272.

Livesley, S.J., Kiese, R., Graham, J., Weston, C.J., Butterbach-Bahl, K., Arndt, S.K., 2008. Trace gas flux and the influence of short-term soil water and temperature dynamics in Australian sheep grazed pastures of differing productivity. Plant Soil 309, 89–103. https://doi.org/10.1007/s11104-008-9647-8.

Lognoul, M., Theodorakopoulos, N., Hiel, M.-P., Regaert, D., Broux, F., Heinesch, B., Bodson, B., Vandenbol, M., Aubinet, M., 2017. Impact of tillage on greenhouse gas emissions by an agricultural crop and dynamics of N2O fluxes: insights from automated closed chamber measurements. Soil Tillage Res. 167, 80–89. https://doi.org/10.1016/j.still.2016.11.008.

Ludwig, B., Wolf, I., Teepe, R., 2004. Contribution of nitrification and denitrification to the emission of N 2O in a freeze-thaw event in an agricultural soil. J. Plant Nutr. Soil Sci. 167, 678–684. https://doi.org/10.1002/jpln.200421462.

Mandl, N., Pinterits, M., Anderson, G., Burgstaller, J., Carmona, G., Danila, A., Emele, L., 2018. Annual European Union Greenhouse Gas Inventory 1990 – 2016 and Inventory Report. Brussels. .

Mappe Fogaing, I., 2013. Mesures Par Spectrométrie Laser Des Flux De N2O Et CH4 Produits Par Les Sols Agricoles. Université de Reims Champagne-Ardenne.

Mathieu, O., Lévêque, J., Hénault, C., Milloux, M.J., Bizouard, F., Andreux, F., 2006. Emissions and spatial variability of N2O, N2 and nitrous oxide mole fraction at the field scale, revealed with 15N isotopic techniques. Soil Biol. Biochem. 38, 941–951. https://doi.org/10.1016/j.soilbio.2005.08.010.

Mauder, M., Foken, T., 2006. Impact of post-field data processing on eddy covariance flux estimates and energy balance closure. Meteorol. Z. 5, 597–609.

Merbold, L., Eugster, W., Stieger, J., Zahniser, M., Nelson, D., Buchmann, N., 2014. Greenhouse gas budget (CO2, CH4and N2O) of intensively managed grassland following restoration. Glob. Change Biol. 20, 1913–1928. https://doi.org/10.1111/gcb.12518.

Mishurov, M., Kiely, G., 2011. Gap-filling techniques for the annual sums of nitrous oxide fluxes. Agric. For. Meteorol. 151, 1763–1767. https://doi.org/10.1016/j.agrformet.2011.07.014.

Molodovskaya, M., Singurindy, O., Richards, B.K., Warland, J., Johnson, M.S., Steenhuis, T.S., 2012. Temporal variability of nitrous oxide from fertilized croplands: hot moment analysis. Soil Sci. Soc. Am. J. 76, 1728–1740. https://doi.org/10.2136/sssaj2012.0039.

Moureaux, C., Debacq, A., Bodson, B., Heinesch, B., Aubinet, M., 2006. Annual net ecosystem carbon exchange by a sugar beet crop. Agric. For. Meteorol. 139, 25–39. https://doi.org/10.1016/j.agrformet.2006.05.009.

Moureaux, C., Ceschia, E., Arriga, N., Béziat, P., Eugster, W., Kutsch, W., Pattey, E., 2012. Eddy covariance measurements over crops. In: Aubinet, M., Vesala, T., Papale, D. (Eds.), Eddy Covariance: A Practical Guide to Measurement and Data. Springer, New-York, pp. pp. 319–331.

Mutegi, J.K., Munkholm, L.J., Petersen, B.M., Hansen, E.M., Petersen, S.O., 2010. Nitrous oxide emissions and controls as influenced by tillage and crop residue management strategy. Soil Biol. Biochem. 42, 1701–1711. https://doi.org/10.1016/j.soilbio.2010.06.004.

Myhre, G., Shindell, D., Bréon, F.-M., Collins, W., Fuglestvedl, J., Huang, J., Koch, D., Lamarque, J.-F., Lee, D., Mendoza, B., Nakajima, T., Robock, A., Stephens, G., Takemura, T., Zhang, H., 2013. Anthropogenic and Natural Radiative Forcing. Climate Change 2013: The Physical Science Basis. Contribution of Working Group I to the Fifth Assessment Report of the Intergovernmental Panel on Climate Change. https://doi.org/10.1038/446727a.

Nemitz, E., Mammarella, I., Ibrom, A., Aurela, M., Burba, G.G., Dengel, S., Gielen, B., Grelle, A., Heinesch, B., Herbst, M., Hörtnagl, L., Klemedtsson, L., Lindroth, A., Lohila, A., Mcdermitt, D.K., Meier, P., Merbold, L., Nelson, D., Nicolini, G., Nilsson, M.B., Peltola, O., Rinne, J., Zahniser, M., 2018. Standardisation of eddy-covariance flux measurements of methane and nitrous oxide. Int. Agrophys. 32, 517–549. https://doi.org/10.1515/intag-2017-0042.

NOAA (National Oceanic and Atmospheric Administration), n.d. Nitrous Oxide (N2O) — Combined Data Set [WWW Document]. URL https://www.esrl.noaa.gov/gmd/hats/combined/N2O.html (Accessed 5.10.2018).

Plaza-Bonilla, D., Álvaro-Fuentes, J., Arrúe, J.L., Cantero-Martínez, C., 2014. Tillage and nitrogen fertilization effects on nitrous oxide yield-scaled emissions in a rainfed Mediterranean area. Agric. Ecosyst. Environ. 189, 43–52. https://doi.org/10.1016/j.agee.2014.03.023.

Portmann, R.W., Daniel, J.S., Ravishankara, a.R., 2012. Stratospheric ozone depletion due to nitrous oxide: influences of other gases. Philos. Trans. R. Soc. B. Biol. Sci. 367, 1256–1264. https://doi.org/10.1098/rstb.2011.0377.

Pugesgaard, S., Petersen, S.O., Chirinda, N., Olesen, J.E., 2017. Crop residues as driver for N2O emissions from a sandy loam soil. Agric. For. Meteorol. 233, 45–54. https://doi.org/10.1016/j.agrformet.2016.11.007.

Reinsch, T., Loges, R., Kluß, C., Taube, F., 2018. Renovation and conversion of permanent grass-clover swards to pasture or crops: Effects on annual N2O emissions in the year after ploughing. Soil Tillage Res. 175, 119–129. https://doi.org/10.1016/j.still.2017.08.009.

Roelandt, C., Dendoncker, N., Rounsevell, M., Perrin, D., Van Wesemael, B., 2007. Projecting future N2O emissions from agricultural soils in Belgium. Glob. Change Biol. 13, 18–27. https://doi.org/10.1111/j.1365-2486.2006.01273.x.

Sabbatini, S., Mammarella, I., Arriga, N., Graf, A., Hörtnagl, L., Ibrom, A., Mauder, M., Merboldt, L., Metzger, S., Montagnani, L., Pitacco, A., Sedlak, P., Šigut, L., Vitale, D., Papale, D., 2016. Protocol on Processing of Eddy Covariance Raw Data.

Seidel, A., Pacholski, A., Nyord, T., Vestergaard, A., Pahlmann, I., Herrmann, A., Kage, H., 2017. Effects of acidification and injection of pasture applied cattle slurry on ammonia losses, N2O emissions and crop N uptake. Agric. Ecosyst. Environ. 247, 23–32. https://doi.org/10.1016/j.agee.2017.05.030.

Shurpali, N.J., Rannik, Ü., Jokinen, S., Lind, S., Biasi, C., Mammarella, I., Peltola, O., Pihlatie, M., Hyvönen, N., Räty, M., Haapanala, S., Zahniser, M., Virkajärvi, P., Vesala, T., Martikainen, P.J., 2016. Neglecting diurnal variations leads to uncertainties in terrestrial nitrous oxide emissions. Sci. Rep. 6, 1–9. https://doi.org/10.1038/srep25739.

Sleutel, S., de Neve, S., Hofman, G., 2003. Estimates of carbon stock changes in Belgian cropland. Soil Use Manag. 19, 166–171. https://doi.org/10.1079/SUM2003187.

Smith, Ka., Ball, T., Conen, F., Dobbie, K.E., Massheder, J., Rey, a., 2003. Exchange of greenhousegases between soil and atmosphere: interactions of soil physical factors and biological processes. Eur. J. Soil Sci. 54, 779–791. https://doi.org/10.1046/j.1365-2389.2003.00567.x.

StatBel, 2018. L'Agriculture Belge En Chiffres [WWW Document]. URL https://statbel.fgov.be/sites/default/files/files/documents/landbouw/FR_Kerncijferslandbouw_2018_Web.pdf (Accessed 10.3.2018).

Taylor, J., 1989. Propagation of uncertainties. An Introduction to Error Analysis: The Study of Uncertainties in Physical Measurements 45–92.

Theodorakopoulos, N., Lognoul, M., Degrune, F., Broux, F., Regaert, D., Muys, C., Heinesch, B., Bodson, B., Aubinet, M., Vandenbol, M., 2017. Increased expression of bacterial amoA during an N2O emission peak in an agricultural field. Agric. Ecosyst. Environ. 236, 212–220. https://doi.org/10.1016/j.archger.2004.12.001.

Theurer, J.C., 1979. Growth patterns in sugarbeet production. J. Am. Soc. Sugar Beet Technol. 20, 343–367.

Trost, B., Prochnow, A., Drastig, K., Meyer-Aurich, A., Ellmer, F., Baumecker, M., 2013. Irrigation, soil organic carbon and N2O emissions. A review. Agron. Sustainable Dev. 33, 733–749. https://doi.org/10.1007/s13593-013-0134-0.

Ussiri, D., Lal, R., 2013. The role of nitrous oxide on climate change. Soil Emission of Nitrous Oxide and Its Mitigation. Springer, pp. pp. 1–28. https://doi.org/10.1007/978-94-007-5364-8.

Van Zwieten, L., Kimber, S.W.L., Morris, S.G., Singh, B.P., Grace, P.R., Scheer, C., Rust, J., Downie, a.E., Cowie, a.L., 2013. Pyrolysing poultry litter reduces N2O and CO2 fluxes. Sci. Total Environ. 465, 279–287. https://doi.org/10.1016/j.scitotenv.2013.02.054.

Vian, J.F., Peigne, J., Chaussod, R., Roger-Estrade, J., 2009. Effects of four tillage systems on soil structure and soil microbial biomass in organic farming. Soil Use Manage. 25, 1–10. https://doi.org/10.1111/j.1475-2743.2008.00176.x.

Vickers, D., Mahrt, L., 1997. Quality control and flux sampling problems for tower and aircraft data. J. Atmos. Ocean. Technol. 14, 512–526. https://doi.org/10.1175/1520-0426(1997)014<0512:QCAFSP>2.0.CO;2.

Wang, B., Brewer, P.E., Shugart, H.H., Lerdau, M.T., Allison, S.D., 2018. Soil aggregates as biogeochemical reactors and implications for soil-atmosphere exchange of greenhouse gases-a concept. Glob. Chang. Biol. 373–385. https://doi.org/10.1111/gcb.14515.

Wilczak, J.M., Oncley, S.P., Stage, Sa., 2001. Sonic anemometer tilt correction algorithms. Bound.-Layer Meteorol. 99, 127–150. https://doi.org/10.1023/A:1018966204465.

Žurovec, O., Sitaula, B.K., Čustović, H., Žurovec, J., Dörsch, P., 2017. Effects of tillage practice on soil structure, N2O emissions and economics in cereal production under current socio-economic conditions in central Bosnia and Herzegovina. PLoS One 12, 1–22. https://doi.org/10.1371/journal.pone.0187681.